Investigating the Effects of Population Growth and Urban Fabric on the Simulation of a 3D City Model

Rani El Meouche[1(✉)], Mojtaba Eslahi[1(✉)], and Anne Ruas[2]

[1] Institut de Recherche en Constructibilité (IRC), ESTP Paris, 94230 Cachan, France
{relmeouche,meslahi}@estp-paris.eu
[2] LISIS/IFSTTAR, Université de Marne-la-Vallée, 77420 Champs-sur-Marne, France
anne.ruas@ifsttar.fr

Abstract. Urbanization induces almost irreversible changes and leads to the phenomenon of urban sprawl and, therefore an increase in artificial lands that affects biodiversity, ecosystems and climate impacts. SLEUTH as a Cellular Automaton (CA) simulation model is widely used by the researchers and urban planners in order to simulate the urban sprawl as a dynamic system. However, SLEUTH, like many other urban simulation models, only considers historical data, and the growth of urban population and urban tissue is not explicitly contemplated and does not have much effect on the simulation results. In this research, we have added these two parameters to SLEUTH and simulated a 3D city model in order to see the impacts of population growth and types of construction on urban sprawl, and to improve the results of simulations. The 3D representation of urban forecasting is based on the results of 2D urban growth simulation while respecting some restrictions on urbanization such as the direction of the footprints, and the distances to urban entities and geographic features. The aim of this research is not only to produce a 3D city model, but also to use the potential of the third dimension to provide different urban future scenarios that can inform prospective strategies for sustainable urban development. The findings allow proposing a set of different simulations that correspond to the different land priorities and constraints, and provide disparate images of city of tomorrow for its application in urban policy as well as smart city modelling and management.

Keywords: Urban sprawl · CA (cellular automata) model · SLEUTH · GIS · 3D city modelling

1 Introduction

1.1 Urbanization and Urban Growth Modelling

The process of increasing the size of cities is called urbanization. Urbanization is mainly occurring due to the population growth, rural exodus and life style, and often make the irreversible changes. In recent decades, much research has been done on the simulation

M. Ben Ahmed et al. (Eds.): SCA 2020, LNNS 183, pp. 1344–1358, 2021.
https://doi.org/10.1007/978-3-030-66840-2_102

of urban growth as a dynamic system, and among the various methods of urban simulation, CA (cellular automata) models are more common for their applications in urban areas due to their simple integration with GIS (Geographic Information System) and RS (Remote Sensing) data. A cellular automaton is a bottom-up and discrete dynamic spatial model. In CA models, the transition rules represent the process of changing each cell state according to the current state of the cell and the states of the cells in its neighborhood [1]. CA models can truly simulate the urban sprawl mechanisms, urban planning theories and urbanization effects [2–4]. Here, we used the SLEUTH urban growth model. SLEUTH is a pattern-based model that uses cellular automaton and terrain mapping and it is widely used to simulate the urban growth [5, 6]. The acronym of SLEUTH is derived from its input maps, including Slope, Land use, Exclusion, Urban, Transportation and Hillshade. The SLEUTH model has evolved over the years and various versions of this model have been proposed to improve the results and reduce the complexity of the model in the calibration and forecasting phases. Goldstein (2004) developed the Genetic Algorithm (GA), which uses a new calibration mechanism instead of the traditional brute force, which reduces calibration time [7]. Dietzel and Clarke (2007) developed an Optimal SLEUTH Metric (OSM) that processes thirteen parameters to find the best coefficients in calibration mode [8]. In 2010, Guan and Clarke developed a parallel version of SLEUTH (pSLEUTH), which uses an open source general-purpose parallel raster processing programming library (pRPL) [9]. This reduces the computational performance of the model during the simulation and calibration process by reducing the computation time for the calibration process with multiple processors. Jantz et al. (2010) used the SLEUTH-3r model to execute a forecasting scenario composed by sub-periods with different spatial dynamics. Their simulations can show the contribution of each of the urban growth patterns according to the scenario hypothesis [10]. In SLEUTH calibration process, several historical maps, such as urban and transportation are needed, nevertheless the rhythm of growth is considered by means of historical data and the model produces the forecasting urban maps with the same tendency as today. In addition, its results are limited to some raster data on which the urbanization is supposed to occur and it is difficult to interpret for decision makers. In this research, we have added more parameters and have explicitly considered the population and building classes to optimize the model. Furthermore, we have provided a 3D representation of the model while respecting some restrictions on urbanization such as the direction of the buildings to the roads, and the distances from the urban entities and the geographic features.

1.2 3D City Modelling

In recent years, governments, municipalities and companies have shown great interest in building virtual models of cities in 3D. A 3D city model can be used in different aspects of urban planning and management in a smart city. A 3D urban model can be used to support the risk management such as emergency response and planning of evacuation [11] as well as in forecasting seismic damage [12] and flooding [13]. In addition, it is used in smart city mobility, operational cost savings, increased resilience and improved sustainability. 3D city model simulations can be used to estimate solar radiation, estimate energy demand and energy efficiency, estimate cast shadows with urban features, estimate noise emission in a restricted environment, and lighting simulations [14]. To

select the most appropriate 3D modelling technique, factors such as data availability, performance accuracy, efficiency, speed and human capital, and costs must be considered. There are many different techniques for producing a 3D city model, such as 3D building of urban footprints and 3D reconstruction and data integration used in the integration of photogrammetry or laser scanning with GIS data. In this research, 3D buildings are created by giving third dimensions to the 2D footprint of buildings. The third dimension represents the height of a building obtained from urban fabric scenarios according to type of building and population density.

In this research, we aim to provide the different scenarios for future urban growth resulting from today's urban planning that conform to different priorities and land constraints, so that it can inform prospective development strategies for sustainable cities that are the foundation of smart city development.

In the next section, the study area is presented. The process and methodology are defined in Sect. 3. In Sect. 4, the urban growth simulations results are shown and discussed. A 3D visualization of the urban growth model is provided in this section. The paper is concluded in Sect. 5.

2 Study Area

In this paper, we present the application of the model in a small study area called Rieucros (43°05′07″ N, 1°46′04″ E) which is a community in a rural area and is located in the department of Ariege in south of Toulouse, France. We select this area due to its small scale which makes it less complicated to model as well as to study the effects and contributions of various factors on it. In addition, a significant increase in the area and rate of population growth has been observed in the last two decades.

The study area is 400 hectares with a population of 686 people (INSEE - national institute of statistics and economic studies, France, 2016). We have used the geospatial database and GIS to create the input maps of SLEUTH. The input maps are the raster data of 100 × 100 pixels, where a cell corresponds to 20 m × 20 m (~400 m^2) on the ground. For this research, we have created urban, land use, excluded and transportation maps from BD TOPO and BD ORTHO of IGN (national institute of geographic information and forestry) database for the year 2017. The slope and hillshade maps are derived from Digital Elevation Model (DEM) of RGE ALTI with a spatial resolution of 5 m, provided by IGN. We have calculated the compound annual population growth rate (extracted from INSEE) and the average population for the coming years, and have defined the building classification as supplementary parameters to add to SLEUTH in order to achieve results that are more reliable.

3 Model Procedure and Methodology

In this research, the data of 2017 is used in order to simulate the urban growth forecast for 2050. In SLEUTH model, a growth cycle is the basic unit of SLEUTH execution and therefore a simulation is composed of 33 growth cycle (from 2017 to 2050). In the proposed method, an urban growth scenario considering environmental constraints, e.g. waterbodies, vegetation areas and forest, is defined. As we discussed before, the

rhythm of growth in SLEUTH is based on the historical data and the impacts of the population growth and the types of the buildings, and as a result the density is not explicitly considered in this model. Furthermore, the SLEUTH results are limited to some raster data which represents the growth areas. To overcome these limitations, two more data i.e. building types and population are added to the model, and different sprawl scenarios are defined as urban fabric scenarios. Later, 3D representations of the urban fabric scenarios are provided considering some urban constraints. Figure 1 illustrates the model procedure.

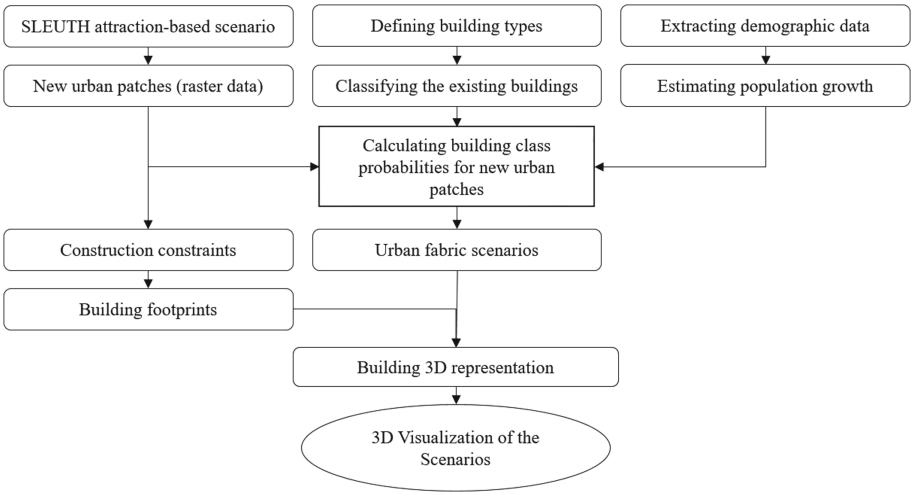

Fig. 1. Method procedure

3.1 SLEUTH Simulation Urban Growth

Structure of the SLEUTH Model. SLEUTH as a cellular automaton model is based on a probabilistic and self-adaptive process that corresponds with only two possible states of the urban or non-urban. The model consists of three process of calibration, forecasting and self-modification. In this model, four spatial growth rules determine and update the growth, including spontaneous growth, new spreading centre growth, edge growth and road-influenced growth. These rules are controlled by five coefficients i.e. dispersion coefficient, breed coefficient, spread coefficient, slope coefficient and road gravity coefficient. These coefficients are specified in the calibration process. In the forecasting process, the model is initialized with the best-fit growth coefficient values that are derived during calibration and the model generates an urban growth map for each growth cycle. The growth cycle begins by giving a unique value to each of the coefficients and then each growth rule is applied and evaluated. A self-modification process controls if the growth rate exceeds or falls below a specific critical threshold.

Attraction-Based Scenario. Using the composition of input layers, we make the possibility of defining the attraction-based scenario for the model, which can improve the overall performance of the model by allowing the inclusion of growth attractors as well as protect the desired zones. The basic excluded maps have the pixel value range from zero to 100. In our model, we have provided an excluded/attractive map. We have defined the pixel value of 50 as neutral value. This makes it possible to define the less or more desirable zones for urbanization in excluded and attractive maps by giving the value more or less than 50, respectively. Therefore, the value of 100 indicates 100% protected areas and the value of zero introduces 100% attractiveness.

Urban Fabric Scenario. We have defined the urban fabric scenarios by integrating the type of buildings and the population on the previous results. We have classified the existing buildings into six different residential categories, by considering their height and configuration. This classification is based on the classification of different kinds of the buildings in a city provided by department of planning and environment of government of Australia. Using demographic information extracted from INSEE, the expected population growth is estimated to be another parameter for model integration. Next, the fictitious urban fabric scenarios are assumed to better understand how a simulated area can be used and for how many residents. Based on the results, a modified urban fabric scenario for enrichment of simulations has been defined.

In fact, in our approach, by defining attraction-based scenario, we have tried to answer the question of where urban expansion is likely to occur, given the environmental constraints. The classification of buildings and the integration of the types of buildings in the model have been done with the aim of answering the question of what kind of buildings may be built in the grown area. By integrating demographic data, we can answer how many inhabitants can be deployed in an urban growth simulation area, or how many buildings are needed to respond to the estimated increase in population.

3.2 3D Representation of Prospective Urban Growth Simulation

In this part, the purpose is to generate a 3D visualization of the simulated urban growth by creating the 3D building representations from the pixels. To do that, first the pixels are transformed from raster data to building footprints. Due to building classification, the current buildings are classified and an average surface for each type of building is calculated. Using the topographic objects such as buildings, rivers, excluded areas and the current buildings a set of constraints are made. Later, the building footprints are created based on these constraints as well as orientation of the buildings to the road. The buildings height for the building footprints are calculated based on the probability of the adjacent neighbours' height considering the probabilities estimated in urban fabric scenarios.

4 3D Urban Growth Simulation

4.1 Attraction-Based Environmental Protection Scenario

An attraction-based scenario is defined by altering the excluded map. As mentioned in Sect. 3, each pixel of the excluded map has a value between 0 and 100. The value 100

indicates 100% protection, value of 50 is neutral and the pixels with value zero are the free zones to build. Therefore, the area that have the value over 50 are resistant to build and the ones under 50 are attractive. An exclusion/attraction map is generated based on the data of 2017. Four concentric zones with different attraction rates make attraction force to the centre. In addition, the areas in distances of seven pixels (~140 m that is obtained experimentally) around water surfaces are considered as attraction areas for dwelling. The excluded areas that are considered in this scenario include remarkable buildings, cemeteries, airfields and sport grounds, railways stations, activity areas (administrative, culture and leisure, education, water management, industrial or commercial, health, sports and transport), water surfaces, national parks and closed forests areas (wood land, closed coniferous forest, closed deciduous forest, mixed closed forest and tree area).

Figure 2 illustrates the exclusion/attraction map. The concentric zones have the distance by the radius of 0.2 km, 0.4 km, 0.6 km, 0.8 km from the centre where their corresponding pixels get the values of 10, 20, 30, 40 respectively, and the remain area gets the value of 50. The historical maps of transportation and urban area for the years of 2000, 2008, 2012, and 2017 are used to calibrate the model.

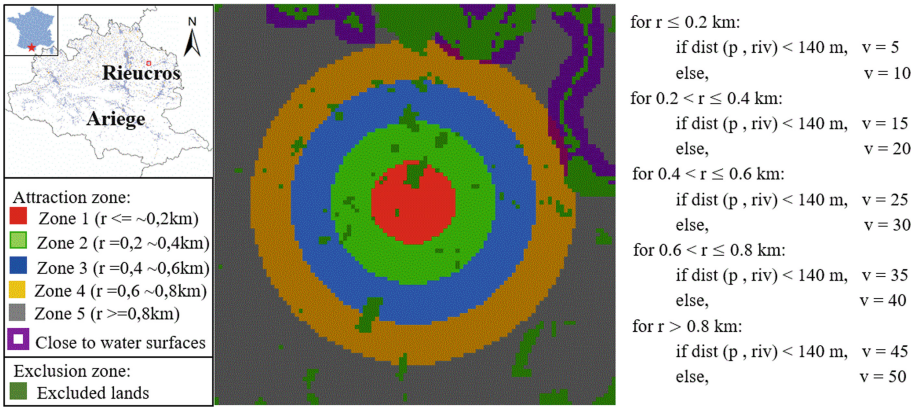

Fig. 2. Exclusion/attraction input map

To obtain the best-fit coefficients for forecasting urban growth, the model is first run in calibration mode. To test and evaluate the model, we first run the model with the input maps of 2000 to simulate the growth for 2017. The results show more than 53% of fits, which is acceptable given the scale of the study area and the size of the pixels. Afterwards, this model is used to produce urban growth maps for 2050 using the forecast mode. The result of the simulation for 2050 are illustrated in Fig. 3.

4.2 Classify the Type of Building

The building classification is done considering the land use and the urban tissue in two parts. First, according to the observations of the study area, two classes of the building are defined including single dwellings and low-rise housing. To do that, the information

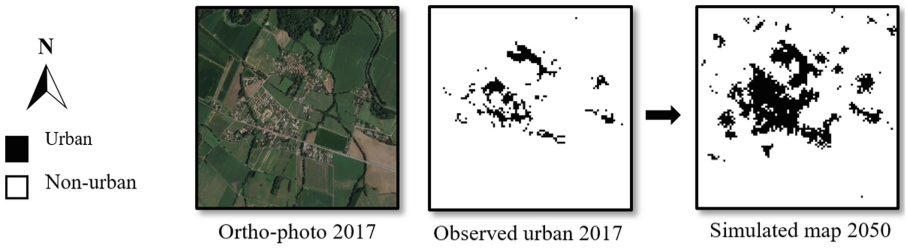

Fig. 3. Urban growth simulated results for 2050

of undifferentiated buildings that are derived from BD TOPO of IGN database are used. The numbers and the height of the buildings are extracted and an average height for each type is calculated. Then, based on the average height of the observed buildings and with respect to the height of the neighbouring buildings and urban fabric scenarios, the appropriate height is given to the new simulated area to represent the new buildings (see Sect. 4.10).

4.3 Estimate the Population Growth

The SLEUTH simulation results are needed to be evaluated by the population density. To integrate the population to our model, it is needed to first estimate the compound annual population rate. The average population growth rate that is estimated for the years between 1999 and 2011 is 1.70% per year. Using growth rate we estimate the forecasting population growth. The average population growth rate for 2050 shows the increasing of 77% of growth. We also estimate average residents in each type of building. This data is used to create the urban fabric scenario.

4.4 Urban Fabric Scenario

Having the building classes, the simulated urban growth and the estimated mean population, we rate the suitable growth cycle to achieve the desired urban fabrics. The purpose of the proposed model is to compare the determinants of urbanization and its measurement in five different cases of urban dispersion as follows:

1. Sprawl urban: The first scenario considers that all new urban patches filled with single dwellings.
2. Medium dense urban: This scenario assumes 80% of the new simulated urban areas are single dwellings and 20% low-rise housing.
3. Medium/high dense urban: This scenario considers 50% of single dwellings and other 50% low-rise housing.
4. High dense urban: In this scenario 30% of buildings specify as single dwellings and other 70% as low-rise housing.
5. Too high dense urban: Last scenario indicates 100% low-rise housing.

These scenarios are fictive and they do not correspond to reality but they help to better understand how this land could be used and how many inhabitants could live in these new areas. Table 1 illustrates the increased population per scenario.

Table 1. Population growth in primary urban fabric scenarios for 2050

Increased population per urban fabric scenarios in 2050	Sprawl urban fabric scenario		Medium dense urban fabric scenario		Medium/high dense urban fabric scenario		High dense urban fabric scenario		Too high dense urban fabric scenario	
	100% single dwelling		80% single dwelling & 20% low-rise housing		50% single dwelling & 50% low-rise housing		30% single dwelling & 70% low-rise housing		100% low-rise housing	
	1 938	283%	2 132	311%	2 423	353%	2 616	381%	2 907	424%

Table 1 shows that all scenarios passed 77% of population growth that is the desired amount of the population increasing estimated for 2050. Based on the obtained results, the urban fabric scenarios are modified to achieve the reliable scenarios. Therefore, we try to find out which growth cycle would match the desired urban fabric better. Three scenarios consist of low dense, medium dense and medium/high dense urban fabrics are modified by their growth cycles of 23rd, 18th and 13th respectively. The medium/high dense urban fabric can accommodate nearly desired population growth while the two other urban fabric scenarios are more sprawl (see Table 2).

Table 2. Population growth in final urban fabric scenarios for 2050

Increased population per urban fabric scenarios in 2050	Low dense urban fabric scenario		Medium dense urban fabric scenario		Medium/high dense urban fabric scenario	
	100% single dwelling		80% single dwelling & 20% low-rise housing		50% single dwelling & 50% low-rise housing	
	23th growth cycle		18th growth cycle		13th growth cycle	
	1 200	175%	1 012	148%	758	110%

4.5 Modifying the SLEUTH Output to Create the Building Footprints

Up to now, we have integrated the exclusion/attraction area, type of buildings and the estimated population growth in our model. We have simulated the 2D urban growth maps by defining the urban fabric scenarios and we know which type of building may be built in which area in the obtained maps. In order to create the 3D representation of the

buildings, it is needed to generate the building footprints. Therefore, we need to consider more parameters such as the distances from the urban entities, geographical features (e.g. water bodies, roads and forest) and current buildings. The SLEUTH outputs include the non-geo-referenced raster data that contains three types of pixels representing the current urban area, new urban area and null pixels. Therefore, we have to first geo-referenced this raster data with respect to our database vector data and then convert them to vector data.

4.6 Positioning and Division of the Building Footprints

The generated polygons are rotated along the closest road section (see Fig. 4). In this step, the roads are divided into small sections, then their directing coefficient is calculated. Later, the angle of orientation of the road section is calculated according to the horizontal axis. The squares that are close to this road section area oriented in related to this angle. The change is made according to the following equation. The angle calculated in the counter clockwise direction.

$$\begin{cases} X = Xc + x\cos\Theta - y\sin\Theta \\ Y = Yc + x\sin\Theta + y\cos\Theta \end{cases} \tag{1}$$

Where (x, y) are the coordinates of the corners expressed in local coordinate system and (X, Y) their associates in global coordinate system. Afterwards, we change the sign of the cosine and sine for the coordinates of four corners.

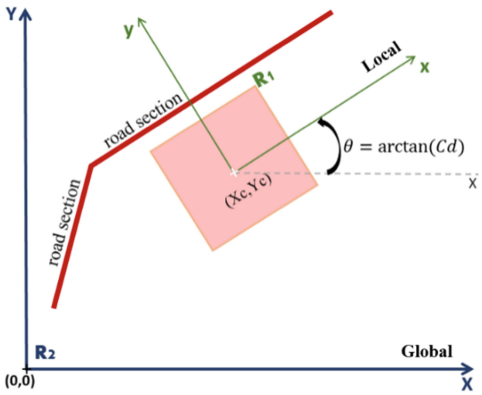

Fig. 4. Orientation of a polygon, R1 and R2 are the local and overall references respectively

We have divided each polygon into four smaller squares to reduce the risk of losing the surfaces while facing to constraints. In this case, if constraints drive the model to delete a polygon, the algorithm will delete a small square that meet the restrictions, instead of whole polygon (see Fig. 5). All these steps are considered in our algorithm and are done automatically.

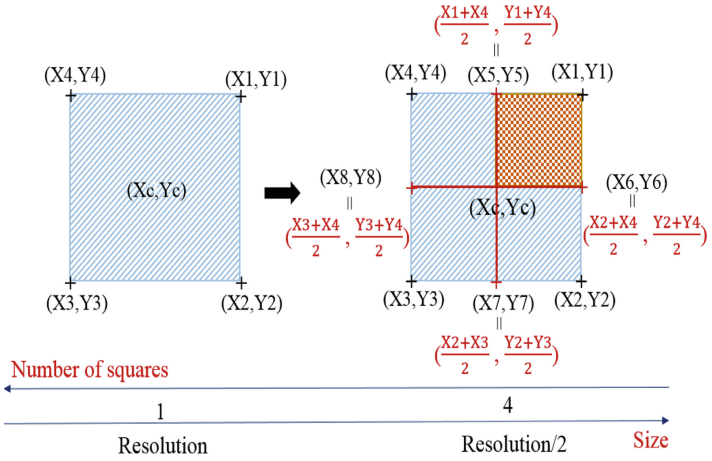

Fig. 5. Subdividing a polygon to smaller squares

4.7 Configuration of the Building Footprints

The adjustment and positioning of the new buildings respect the old buildings. The polygons may overlap after orienting and dividing. Furthermore, adjustment and positioning of new buildings follow the layout of the old buildings and we should define distance between a polygon and different land occupation entities based on old buildings. Overcoming overlaps and respecting the distance to urban units may lead the elimination some parts of polygons. Two types of constraints are taken into account as land occupation entities including:

- Continuous constraints: They have a linear distribution in space including vegetation, water bodies, roads and railways.
- Discrete constraints: They consist of the points or small areas such as remarkable buildings, cemeteries, airfields, sport grounds, activity areas, industrial or commercial areas and existing buildings.

In order to consider the discrete constraints in model, we measure the distance of the current buildings from each other and from other discrete constraints and calculate the average distances. Later, by defining a buffer equal to average distance, the obtained distances to the nearest discrete constraints are applied for each polygon. These buffers might intersect each other or some other entities that should be removed in these cases. When only a part of a polygon intersects a buffer, the subdividing of polygons that we have done before, can help the model not to lose the polygon completely. Furthermore, we have defined a threshold for the intersection of a square to a buffer equal to 30% of a square area. If a buffer overlaps more than 30% with a square, that square will remove. The process for the continuous constraints is based on a double geo-processing buffer:

- First, we measure the distance from the nearest existing building to the continuous constraints and then we make a buffer of ten times of this distance. We assume that all the buildings close to the sections of the continuous constraints are at this distance.
- Next, the average distance of these buildings from a continuous constraint is calculated. This average is considered as a minimum distance for new buildings to these constraints. In applying continuous constraints to the polygon, the algorithm makes a second buffer with a distance equal to the average distance and remove the intersection of this buffer with the polygon.

4.8 Assembles the Polygonal Components

In order to generate the building footprints, the divided squares must be assembled according to the type of building. Therefore, the building footprints will have the surfaces that remains of small squares. Considering the building types and the size of the polygons, a maximum surface (Smax) for each type of a building footprint is defined. The Smax for the single dwelling and low-rise housing are calculated as 156 m^2 and 256 m^2 respectively. We have defined IDs for each polygon that help with the assembly process. In the assembly process, the algorithm controls that the total area does not exceed Smax. If the area of the assembled squares is less than Smax, the whole polygon represents a building. The polygons whose surfaces exceed Smax, are subdivided into smaller polygons, corresponding the decomposition of the pixel into subpixels. In this process, we consider the small squares which belong to same pixel. According to Smax, we can gather them as needed so that both on the left or on the right of the set of small squares of the sub-pixel means LU (Left/Up) with LD (Left/Down) and RU (Right/Up) with RD (Right/Down). In the algorithm, it is defined that the width of a building locates on the roadside and therefore have access to nearest road (see Fig. 6).

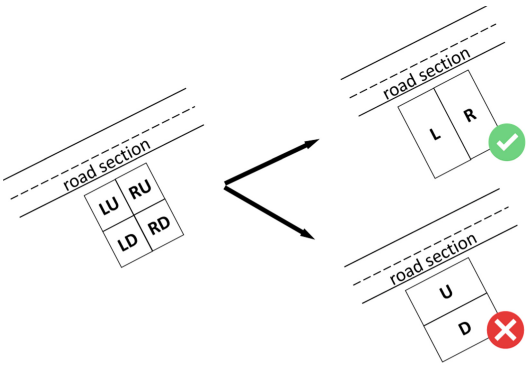

Fig. 6. Assembling sub pixels respecting the roads

4.9 Building Footprints Generation and Positioning the Building Representations

In the assembly process, we gathered the remained components of each polygon and created the new polygons. Different possible types of building footprints are provided

based on urban fabric scenarios. In this step, we apply the appropriate erosion to each polygon that respects the defined area of the building classes, the distance between the new buildings and the Smax and forms the footprints of the building (see Fig. 7).

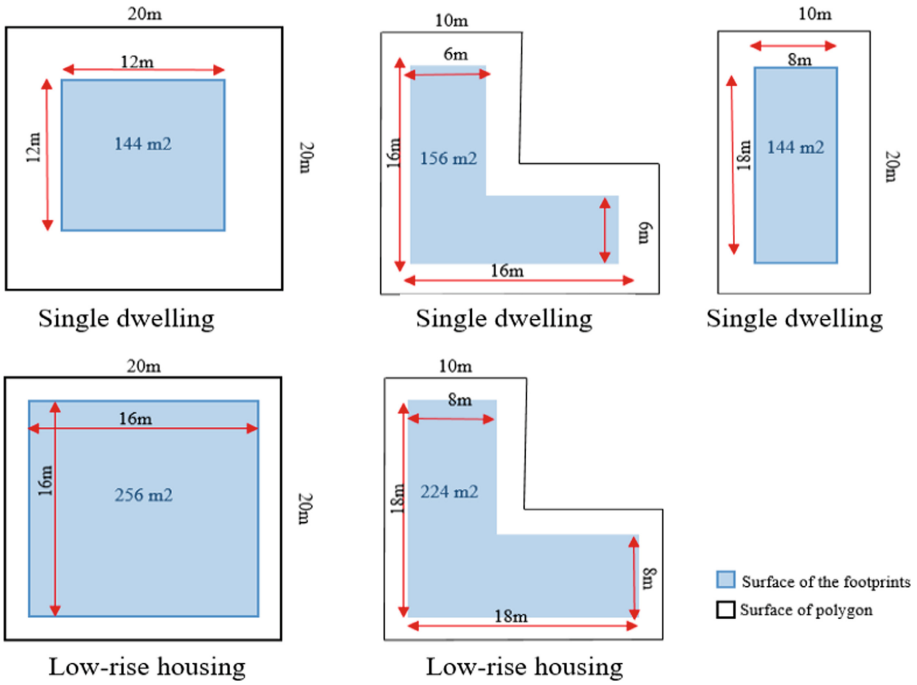

Fig. 7. Erosions performed on polygons according to the type of building. The half-pixel case is not intended for low-rise housing because it cannot provide the required surface for this type of building due to the average area of existing buildings for this type.

4.10 The 3D Visualization of the City

Calculating the suitable height for these footprints according to urban fabric scenario (urban sprawl considering the population growth and types of buildings) will lead to generate the 3D representation of prospective urban model. To find the information of the possible heights for the new buildings and give an appropriate height to the footprints, the height probabilities for each polygon are calculated according to the type of neighbouring buildings. Given the scenarios where it is necessary to have mixed height values, we use an algorithm that combines the random aspect and a statistical interpolation.

The urban fabric of the study area is composed of two types of building including single dwellings and low-rise housing. As mentioned in Sect. 4.2, the average height for each type is calculated. In this step, the algorithm sorts the buildings in ascending order of their surfaces (SB1 $<$ SB2), and calculates the percentages of combination in

different scenarios for each building type of B1 and B2 by Prs1 and Prs2, respectively (see Fig. 8). P1 and P2 indicate the average height probabilities for each building. These parameters are calculated from the nearest current building heights.

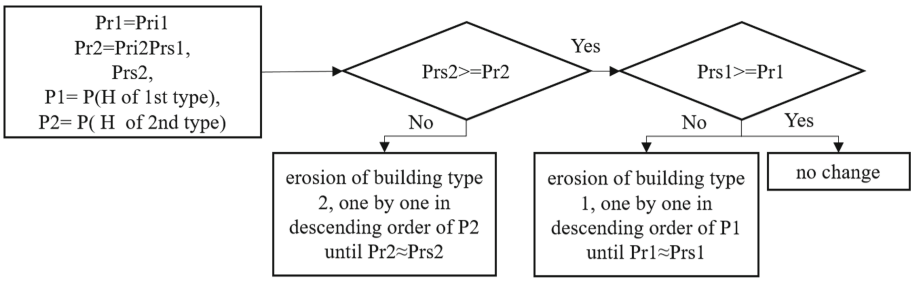

Fig. 8. Algorithm of calculating the probability of the height for each building according to the building types and urban fabric scenario

Two radiuses with the values of r1 and r2 are calculated based on the distance of the nearest neighbour of each existing building by applying the quintile classification. The distance between the new building and the current buildings are calculated (DIS), then the inverse distance (IDIS) and the sum of the inverse distance (SIDIS) are computed. The new buildings are classified according to the distance to the neighbour in three clusters.

- New buildings that have at least one neighbour that is part of the current buildings on a circle (r1)
- New buildings that have at least one neighbour that is part of the current buildings on a limited ring between the small circle (r1) and the large circle (r2)
- New buildings that have no neighbours that are part of the current buildings on a circle (r2)

The impact rate is calculated for each type of building, which affects the type of new building (building with height equal Hi). Then, the total probability of each type associated with each building is deduced, which leads a new Pi that signifies the probability of a building with height Hi. Next, the initial percentage (Pri) of each type of building for the variable percentage (Pr) is calculated. The final step is the illustration of 3D representation of the urban growth model. To do that, a Digital Elevation Model (DEM) using BD TOPO data altitudes (IGN) is created and using the calculated heights, an extrusion of the various layers including new buildings is applied. Figure 9 illustrates the results displayed in ArcScene.

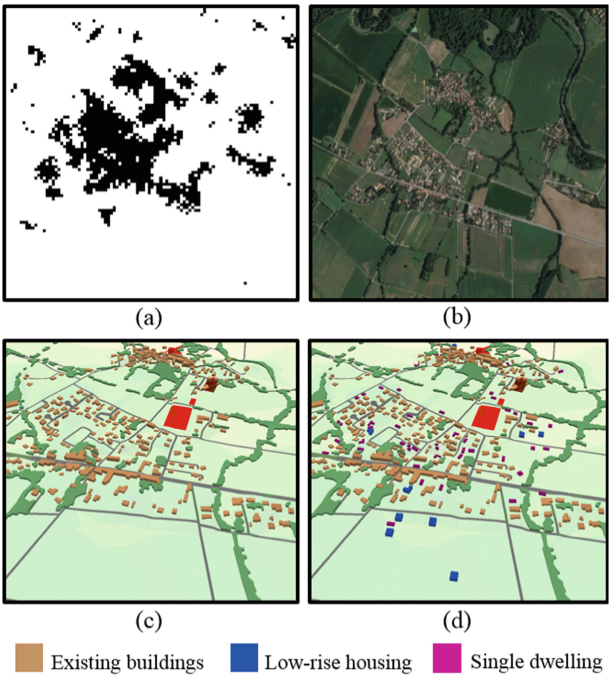

Fig. 9. a) 2D simulated urban map for 2050, (b) Ortho-photo 2017, (c) 3D representation of observed city in 2017, (d) 3D representation of the city for 2050

5 Conclusion

Urban sprawl phenomenon is a big challenge for the authorities and urban planners. The urban simulation techniques are willing to solve the various problems of urban growth modelling. Most of the urban growth models are based on the historical data and they simulate the growth similar to tendency as today. Furthermore, they mostly consider the exclusion area but rarely integrate the attraction zones in the simulation.

In this research, we have generated an attraction-based scenario that leads to integrate both exclusion and attraction areas in the model. We have included the impact of population growth and types of buildings on the urban growth simulation model. This leads to provide the urban fabric scenarios that aims to compare the determinants of the urbanization and its measurement in different scenarios of urban sprawl. These scenarios can also help to understand the difference between scattered and dense growth.

We used the potential of the 3D modelling to provide different urban future scenarios that can inform prospective strategies for sustainable urban development. We have developed a model that can simulate the footprint of buildings in new urban areas and calculate the height of buildings according to the probability of height in the area where the new building is located. We have created a primary 3D model of the simulated area by considering some urban constraints such as distance to urban units and respecting the shape and height of existing buildings. In the created 3D urban growth model, the buildings are illustrated in block models with flat roof structure (similar to LoD1 of CityGML). The

provided 3D model aims to help better understand the simulation results and to facilitate the interpretation of the SLEUTH simulation. The 3D urban growth models can be used in various applications such as pollution estimation, energy demand estimation, solar radiation estimation and traffic management.

References

1. Schiff, J.L.: Cellular Automata: A Discrete View of the World, p. 40. Wiley (2011). ISBN 9781118030639
2. Clarke, K.C., Gaydos, L.J.: Loose-coupling of a cellular automaton model and GIS: long-term growth prediction for the San Francisco and Washington/Baltimore. Int. J. Geogr. Inf. Sci. **12**, 699–714 (1998)
3. Antoni, J.P., Vuidel, G., Omrani, H., Klein, O.: Geographic cellular automata for realistic urban form simulations: how far should the constraint be contained? (2019). https://doi.org/10.1007/978-3-030-12381-9_7
4. Eslahi, M., El Meouche, R., Ruas, A.: Using building types and demographic data to improve our understanding and use of urban sprawl simulation. In: Proceedings of the International Cartographic Association, vol. 2, p. 28 (2019). https://doi.org/10.5194/ica-proc-2-28-2019
5. Clarke, K.C.: A decade of cellular urban modeling with SLEUTH: unresolved issues and problems. In: Brail, R.-K. (ed.) Planning Support Systems for Cities and Region, pp. 47–60. Lincoln Institute of Land Policy, Cambridge (2008)
6. Project Gigalopolis (2018). http://www.ncgia.ucsb.edu
7. Goldstein, N.C.: Brains vs. brawn – comparative strategies for the calibration of a cellular automata–based urban growth model. In: Atkinson, P., Foody, G., Darby, S., Wu, F. (eds.) Geo Dynamics. CRC Press, Boca Raton (2004)
8. Dietzel, C., Clarke, K.C.: Toward optimal calibration of the SLEUTH land use change model. Trans. GIS **11**, 29–45 (2007). https://doi.org/10.1111/j.1467-9671.2007.01031.x
9. Guan, Q., Clarke, K.C.: A general-purpose parallel raster processing programming library test application using a geographic cellular automata model. Int. J. Geogr. Inf. Sci. **24**(5), 695–722 (2010)
10. Jantz, C.A., Goetz, S.J., Donato, D., Claggett, P.: Designing and implementing a regional urban modeling system using the SLEUTH cellular urban model. Comput. Environ. Urban Syst. **34**(1), 1–16 (2010). https://doi.org/10.1016/j.compenvurbsys.2009.08.003
11. Tashakkori, H., Rajabifard, A., Kalantari, M.: A new 3D indoor/outdoor spatial model for indoor emergency response facilitation. Build. Environ. **89**, 170–182 (2015)
12. Christodoulou, S., Vamvatsikos, D., Georgiou, C.: A BIM-based framework for forecasting and visualizing seismic damage, cost and time to repair. In: Proceedings of the European Conference on Product and Process Modelling, Cork, Ireland, 14–16 September (2011)
13. Varduhn, V., Mundani, R.P., Rank, E.: Multi-resolution models: recent progress in coupling 3D geometry to environmental numerical simulation. In: 3D Geoinformation Science, pp. 55–69. Springer, Cham (2015)
14. Biljecki, F., Stoter, J., Ledoux, H., Zlatanova, S., Çöltekin, A.: Applications of 3D city models: state of the art review. ISPRS Int. J. Geo-Inf. **4**, 2842–2889 (2015). https://doi.org/10.3390/ijgi4042842